Gowree, E.R. & Atkin, C.J. (2015). On the turbulent mean-flow at the leading edge of a swept wing. Paper presented at the 50th 3AF International Conference on Applied Aerodynamics, 30 Mar - 01 Apr 2015, Toulouse, France.

CITY UNIVERSITY LONDON

City Research Online

50th 3AF International Conference on Applied Aerodynamics
Toulouse, France, 30-31 March, 1 April, 2015

FP60-2015-Gowree

ON THE TURBULENT MEAN-FLOW AT THE LEADING EDGE OF A SWEPT WING

50th 3AF INTERNATIONAL CONFRENCE ON APPLIED AERODYNAMICS
Toulouse, France, March 30-31, April 1, 2015
Erwin R. Gowree [(1)], Chris Atkin [(2)]

[(1)] City University London, Dept. of Mech. & Aero. Engineering, Northampton Square, London EC1V 0HB, UK, Email: erwin.gowree.2@city.ac.uk
[(2)] City University London, Dept. of Mech. & Aero. Engineering, Northampton Square, London EC1V 0HB, UK, Email: chris.atkin.1@city.ac.uk

ABSTRACT

Due to the presence of a singularity in the governing three-dimensional (3D) momentum integral equation at the attachment line (AL) and numerical issues while marching immediately downstream, a numerical fix was previously imposed in the leading edge (LE) modelling of Airbus Callisto. This technique has been employed for half a century during the design and optimisation of transonic wings, but recent analysis on AL control for form drag reduction rose concerns about this previously accepted numerical fix. An experimental study was conducted to validate this LE approximation. Measurement of the boundary layer integral quantities immediately downstream of the AL showed considerable increment; therefore a modification to the 3D governing equation was suggested to remove the numerical fix in the LE modelling. Comparison with experimental measurements showed that the proposed numerical model is not only able to predict the flow within an agreement of ±5%, but it is also able to capture the non-monotonic behaviour in the development of the momentum thickness in the vicinity of the AL, not reported previously.

1. INTRODUCTION

For aircraft wings operating at high Reynolds number, the flow along the attachment line (AL hereafter) is often turbulent and numerical methods, including low-order CFD codes, need to be able to predict the development of the wing boundary layer flow starting from a turbulent attachment line. Unlike on an unswept wing, the presence of a spanwise velocity component introduces large curvature in the inviscid streamline as the flow is turned from a fully spanwise flow at the AL towards the chordwise direction by the accelerating flow along the curved leading edge (LE). The viscous flow includes a significant crossflow component normal to the external streamline. Modelling the flow in the vicinity of the AL poses significant challenges to the CFD community due to the presence of highly curved streamlines and possibly large turbulence anisotropy arising from the dominant spanwise flow.

Recently interest in low-order CFD has risen due to the ease of incorporating flow control modelling as a replacement for simple data-sheet methods for use in future project studies, for which traditional design rules are not reliable. CVGK is just such a low-order method, coupling the Airbus boundary layer code, Callisto, to the full potential method of Garabedian & Korn [1], extended to handle infinite-swept wing flows using Lock's transformation [2]. Callisto is a 2.5D turbulent boundary layer method based on the von Karman momentum integral equations, incorporating the lag-entrainment model of Green et al. [3], and modelling 3D turbulence using the streamline analogy. CVGK is the latest development of the viscous-inviscid-interaction (VII) method for transonic aerofoil flows originally developed at the Royal Aircraft Establishment [4]. The VII approach is described in detail by Lock & Williams [5], and has the advantage of requiring considerably less computing resource than RANS, with comparable accuracy for attached flows, while intrinsically delivering a breakdown of drag into friction, form and wave drag components. A

recent numerical study conducted by Gowree [6] demonstrated that CVGK can predict the drag on swept wings in transonic flow with acceptable accuracy.

In the case of the turbulent AL, the streamline analogy leads to singular governing equations in a very confined region downstream of the AL as a result of the streamline being locally perpendicular to the co-ordinate along which the boundary layer solver marches. At the AL itself the problem is resolved by invoking local similarity arguments, but immediately downstream of the AL the singularity seemingly cannot be resolved. In CVGK this region has to date been approximated by simply extrapolating the results of the AL calculation to about 0.5% chord downstream.

Due to the lack of detailed measurements in this region it is difficult to benchmark the existing numerical models or derive a more reliable semi-empirical model for the turbulence. Measurement of the turbulent boundary layer at the LE of a swept wing can be an equally challenging task due to the presence of a complex system of three-dimensional (3D) boundary layer, which tends to be very thin as it is at its origin and growing very slowly due to the presence of a favourable pressure gradient. An experimental campaign was launched at the Handley Page Aeronautics Laboratory at City University to investigate the behaviour of the viscous flow in the vicinity of the AL generated on a wing model with very high LE curvature so as to validate and improve the prediction from an in-house boundary layer code.

2. THE EXPERIMENT

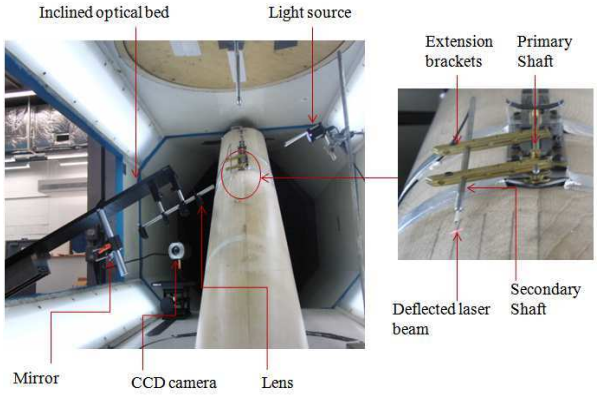

Figure 1: Experimental set-up and hot-wire alignment.

The experimental model used during the test was wooden, with a NACA0050 aerofoil profile, LE radius of curvature of *0.114m*, normal-to-LE chord length of *0.466m* and was swept by *60º*. It was mounted between the floor and ceiling of the test section of the T2 wind tunnel at the Handley Page Laboratory, City University London, as shown in Fig.1. The T2 tunnel has a speed range of 4 to 55 m/s. A surface-mounted boundary layer traverse probe with micro-displacement capability was designed to capture the velocity profile, with a resolution of *2.5μm* per step achievable. Fig. 1 also shows the simple digital optical system used for near-wall alignment of the hot wire sensor and Fig. 2 shows three snap shots of the hot wire support in contact with the surface of the model at three different chordwise locations.

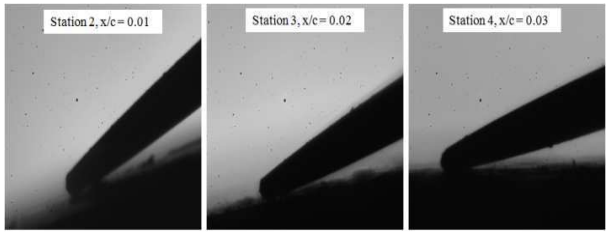

Figure 2: Snapshot of the side of the hot wire support in contact with the surface.

A single normal (SN) hot wire probe, Dantec 55P15, was used to capture the single velocity component at the AL and a single yawed (SY) probe, Dantec 55P12, for the measurement of the two in-plane velocity components downstream of the AL. The constant temperature anemometry (CTA) technique was used and the hot wire probes were connected to the DISA-55M10 CTA Standard Bridge (M-Unit) module, which consists of a Wheatstone bridge equipped with a servo mechanism. The M-Unit was in turn interfaced with a National Instruments (NI)-DAQ card with built-in A/D converter and installed in a PC for data acquisition using NI-Labview. The hot wire output signal was pre-filtered through a low-pass filter rated at 4.8 kHz prior to recording. King's law was applied for the reduction of hot wire output voltage. The calibration of the SN probe and measurement of a single velocity component at the AL was straight forward, but more challenging for the SY probe for the two velocity components measurement downstream. In this case Bradshaw's method described in reference [6] was employed and a yaw calibration was required due to the directional sensitivity of the SY probe.

Preston's [7] technique was employed for the measurement of local surface shear stress. At the AL, the flow resolves into a single, spanwise velocity component, similar to the streamwise flow along a flat plate, thus the method should yield reasonable accuracy. This

technique has been restricted to 2D flows where the skin friction is acting along the same axis as the velocity component; therefore for the flow downstream of the AL an attempt was made to extend this technique to the 3D boundary layer under the highly curved streamline at the LE of a swept wing. The surface shear stress measurement was made by aligning the Pitot-tube in the direction of the local external streamline, obtained from the velocity components at the edge of the boundary layer.

3. EXPERIMENTAL RESULTS

3.1. Streamwise Velocity Profiles

Due to contamination by the turbulent boundary layer on the floor of the wind tunnel, the instability along the AL started to amplify at $R_\theta > 100$. This threshold is in agreement with the results of Pfenninger [8] and Gaster [9]. The turbulent mean velocity profiles were captured at various AL Reynolds numbers and, using the surface shear stress measurements these profiles were represented in wall units, Fig. 3. For the fully turbulent velocity profiles, some measurements were achieved in the laminar sub-layer despite a boundary layer thickness of the order of *3mm*, owing to the digital optical system which enabled alignment of the hot wire probe very close to the wall. Fig. 4 shows that the logarithmic region of the velocity profiles deviates from the universal log-law used by Cumpsty and Head [10], although significant scatter can be seen in the latter's experimental results. In the present work the log-law was modified according to the DNS analysis of Spalart [11] who suggested that, for $R_\theta > 100$, the log-law was defined by the von Karman constant, $k < 0.41$.

The mean streamwise velocity profiles captured downstream of the AL are presented in Fig 4, for an AL Reynolds number, $R_\theta = 590$. The good agreement between the port and starboard side measurements demonstrates that the AL was at $x/c = 0$ as the model was symmetrical and at zero incidence. Using the surface shear stress measurements the velocity profiles were represented in wall units as shown in Fig. 5. The inner region of the velocity profiles matched the 'universal log-law' with reasonable agreement, but the measurements in the viscous sub-layer does not show any trend with chordwise position. At $x/c=0.02$, for $y^+ \approx 10$ the first couple of data points remains more or less constant, unlike the profiles at the remaining chordwise locations and this might be due to the inability of capturing the flow very accurately near the wall. However, the agreement with the universal log-law suggests that the profiles were captured with reasonable accuracy and be used for further analysis.

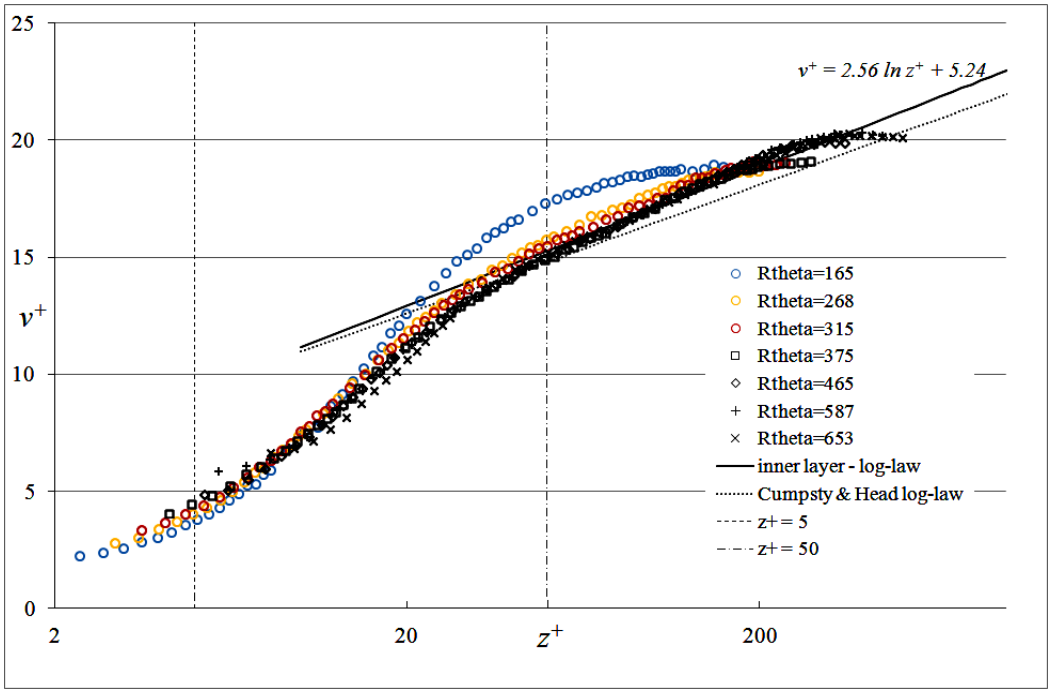

Figure 3: The turbulent velocity profile at the AL.

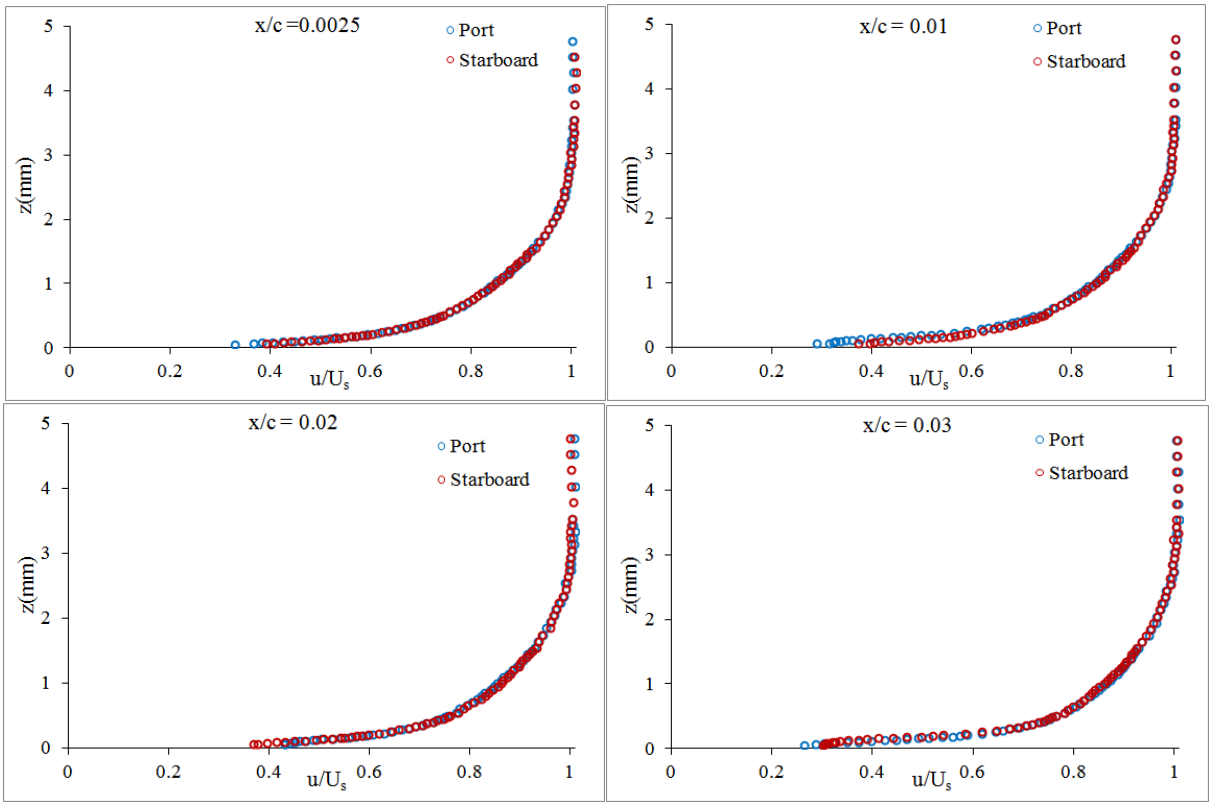

Figure 4: Streamwise velocity profiles at the LE for an AL $R_\theta = 590$.

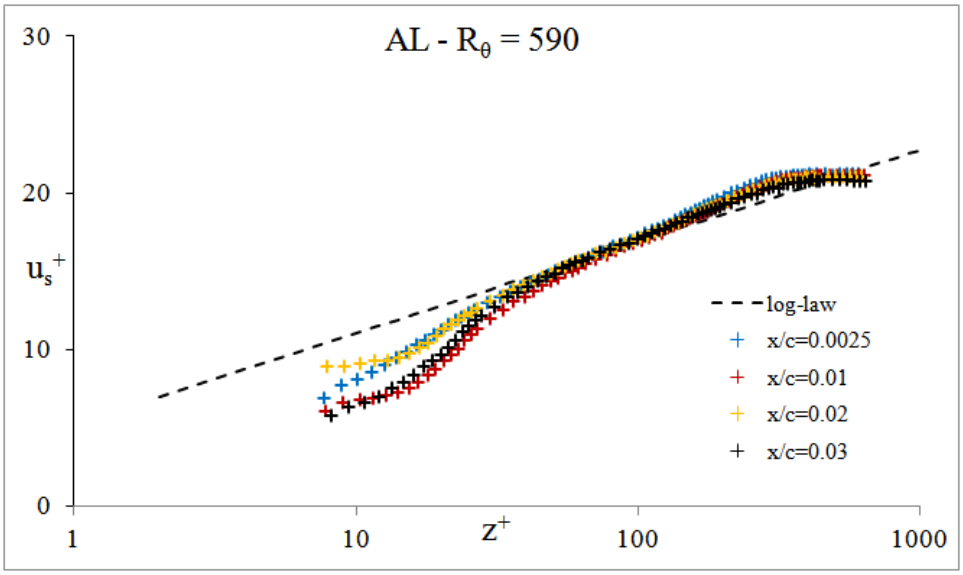

Figure 5: Streamwise velocity profiles in wall units, downstream of the AL at $R_\theta = 590$.

3.2. Crossflow Velocity Profiles

Fig. 6 shows the crossflow velocity profiles at different chordwise positions downstream of the AL. A good agreement can be observed between the port and starboard measurement except at *x/c = 0.03*. This was due to the limitation in the yaw sensitivity of the SY probe and was therefore restricted to ±*70°* during the yaw calibration. More details of the crossflow was revealed when they were plotted on the triangular hodograph model proposed by Johnston [12], as shown in Fig. 7 where the normalised crossflow velocity can be represented as a function of streamwise velocity. From Fig. 7 it is easier to identify the

point where the crossflow changed direction or in other words the formation of the 'S-type' or 'cross-over' crossflow profiles at *x/c > 0.002*5. Normally, the cross-over point occurs very close to the wall and shifts upwards further downstream, as observed in Fig. 7. Due to restriction in near wall measurement it is difficult to capture the chordwise location where the cross-over is incipient. The main issue with the triangular representation is the difficulty in applying a linear fit to the profiles especially around the curvature near the extremity of the crossflow velocity.

According to Johnston the angle between the limiting and the external streamline, β, can be approximated as the gradient of the line of best fit connecting the origin and the apex of the triangle which are stationary points (maxima or minima) of the velocity profiles and is assumed to be the region where the surface shear stress is dominant. Using this approach, on the port side of the model, at *x/c=0.0025*, the angle between the limiting and external streamline, $\beta = -4.9°$. The same method applies to the cross-over profile, but due to insufficient data in the near wall region for the measurement between *x/c=0.01-0.02* it was not possible to determine β until *x/c=0.03,* where the apex of the triangle could be resolved. At this position the angle was calculated as $\beta = -5.9°$. From Fig. 7 the cross-over in the crossflow profiles started immediately downstream of *x/c=0.0025*, this meant that β did not increase to large negative values and as a matter of fact the wall shear stress changed direction. Therefore, it is fair to assume that within the current experimental domain the limiting streamline angle ranged between $-5° < \beta < 6°$

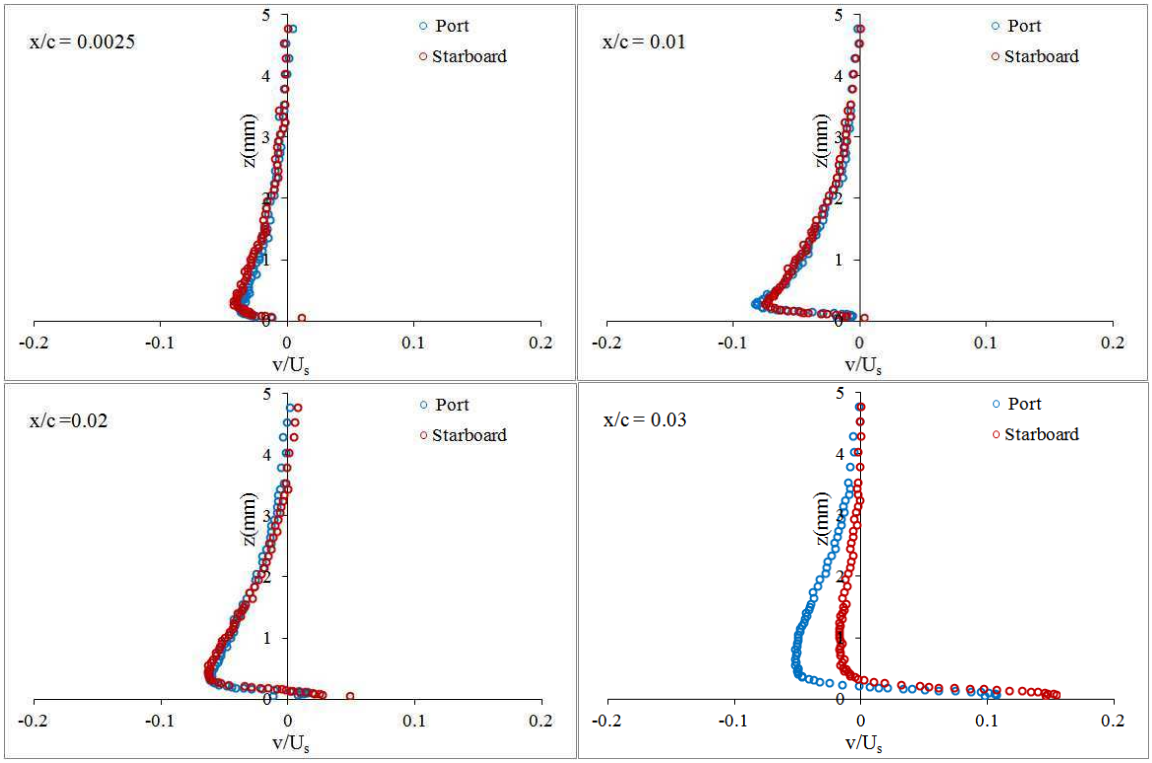

Figure 6: Crossflow velocity profiles downstream of the AL at $R_\theta = 590$.

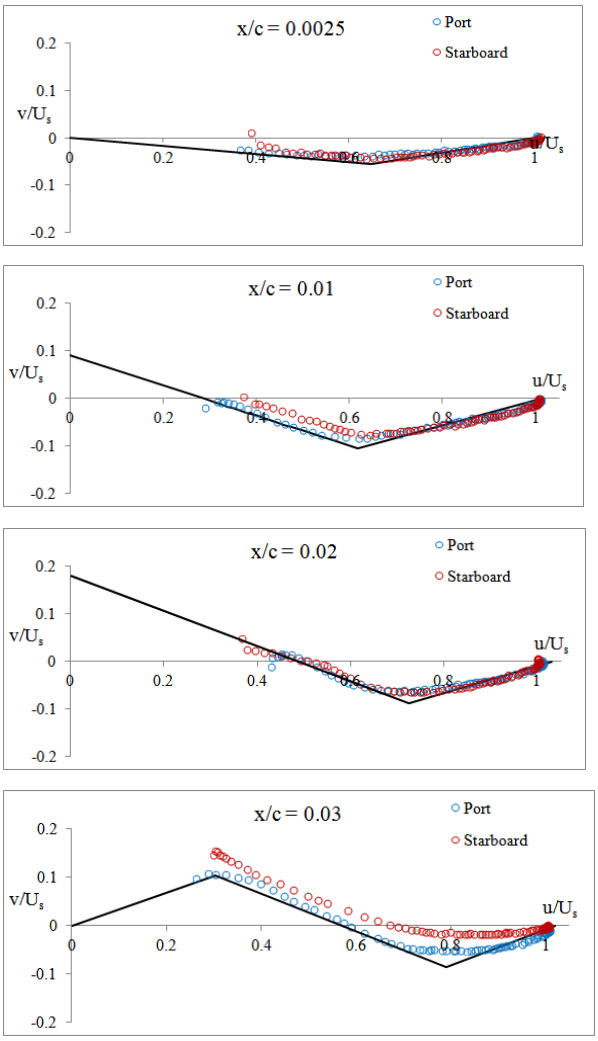

Figure 7: Triangular representation of crossflow profiles using Johnston's model.

3.3. Topology of the flow at the Leading Edge

The external inviscid streamline can be resolved in terms of the chordwise and spanwise velocity components at the edge of the boundary layer. These can be determined from the measurements of the SY probe which is inherently sensitive to flow directions. The development of the external streamline is plotted in Fig. 8, which shows the variation in streamline divergence angle, ψ with respect to the chord normal to the LE at several chordwise position. At $x/c = 0.0$, $\psi \approx 90°$ as the flow along the AL is purely spanwise and at $x/c > 0.03$ the external streamline starts to align itself with the direction of the freestream flow as the effective sweep angle was determined to be approximately $63°$.

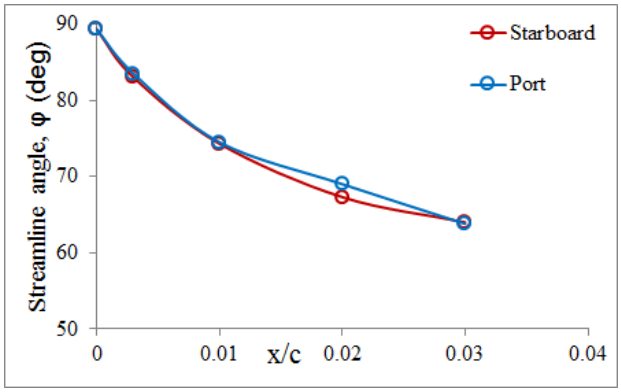

Figure 8: The orientation of the external streamline with respect to the chord normal to the LE at an AL of $R_\theta = 590$.

The streamwise and crossflow boundary layer integral quantities in an incompressible 3D boundary layer can be defined as,

$$\delta_1^* = \int_0^\delta \left(1 - \frac{u}{U_s}\right) dz, \quad \delta_2^* = -\int_0^\delta \frac{u}{U_s} dz$$

$$\theta_{11} = \int_0^\delta \frac{u}{U_s}\left(1 - \frac{u}{U_s}\right) dz, \qquad \theta_{21} = \int_0^\delta \frac{uv}{U_s^2} dz$$

$$\theta_{12} = \int_0^\delta \frac{u}{U_s}\left(1 - \frac{u}{U_s}\right) dz, \quad \theta_{22} = \int_0^\delta \frac{u^2}{U_s^2} dz$$

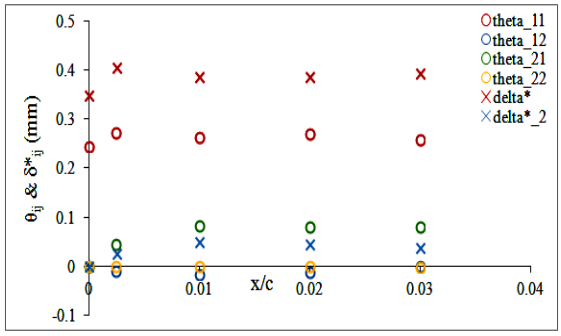

Figure 9: The port side streamwise and crossflow integral quantities in the vicinity of the AL at $R_\theta = 590$

Using the streamwise and crossflow velocity profiles captured experimentally the integral quantities were estimated and their development in the vicinity of the AL is presented in Fig. 9. The streamwise momentum thickness, θ_{11} increases by approximately 15% immediately downstream of the AL and so does the streamwise displacement thickness, δ_1^*. A slight non-monotonic behaviour can be observed in the development of θ_{11} and δ_1^*, but this effect might also be due to experimental inaccuracies. The crossflow momentum thicknesses, θ_{11} and θ_{12} are almost negligible

at the AL (equal to zero in theory) and do not vary significantly downstream, but θ_{21} and δ_2^* attain a value of approximately 35% of the streamwise displacement and momentum thicknesses respectively. This increment in the integral quantities is significant and is not captured by the LE approximation in Callisto.

4. THE NUMERICAL MODELLING IN CALLISTO

4.1. Governing Equations

The numerical approach employed during the computational of a fully turbulent boundary layer along an infinite-swept wing using CVGK was presented in Atkin and Gowree [13] and in a simplified form the governing 3D momentum integral equations, entrainment equations coupled with the velocity transpiration equation can be expressed in a matrix system as

$$\begin{bmatrix} A_\theta & A_{\bar{H}} & A_\beta & A_U \\ E_\theta & E_{\bar{H}} & E_\beta & E_U \\ N_\theta & N_{\bar{H}} & N_\beta & N_U \\ W_\theta & W_{\bar{H}} & W_\beta & W_U \end{bmatrix} \frac{d}{d\xi} \begin{bmatrix} \theta \\ \bar{H} \\ \beta \\ U_e \end{bmatrix} = \begin{bmatrix} A_0 \\ E_0 \\ N_0 \\ W_0 \end{bmatrix} \quad (1)$$

The terms A and N denote the coefficients of the streamwise and normal momentum integral equations and E and W denote the entrainment and transpiration equations respectively. θ, $\bar{H}$, β, U_e and ξ are the momentum thickness, transformed shape factor, the angle between the external and limiting streamline, the velocity at the edge of the boundary layer and the streamwise coordinate respectively. For the full definition of these parameters the readers are referred to Atkin [13] or Gowree [6].

4.2. Previous Leading Edge Approximation

The progression of the external inviscid streamline in the vicinity of the AL is presented schematically in Fig. 1. At the AL the streamline divergence angle, ψ, is equal to $\pi/2$ and as the skin friction is acting parallel to the AL, the angle between the limiting and the external streamline, β, is zero. Following the necessary substitution in the governing equations

$$A_\theta = A_{\bar{H}} = A_\beta = A_U = 0$$

$$E_\theta = E_{\bar{H}} = E_\beta = E_U = 0 \quad (2)$$

$$N_\theta = N_{\bar{H}} = N_\beta = N_U = 0$$

$$W_\theta = W_{\bar{H}} = W_\beta = W_U = 0$$

This leads to a singularity in the governing equations at the AL. Therefore in Callisto, Smith's [14] formulation of the AL governing momentum integral equations is employed to initialise the boundary layer at the AL.

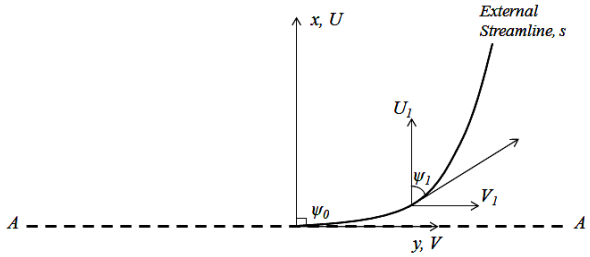

Figure 10: The inviscid flow in the vicinity of the AL.

However the numerical issue persists downstream of the AL as ψ remains close to $\pi/2$ and β is very small, although the conditions for Smith's self-similar solution [15] no longer apply. A crude fix is to extrapolate the attachment line solution until a chordwise position downstream where $\psi \leq 80°$, sacrificing accuracy for robustness. Similar difficulties were encountered by Thompson and McDonald [16] and later by Smith [15] and a numerical fix similar to that in Callisto was adopted. For most practical cases this approximated region accounts for less than *1%* of the chord length and it has thus far been assumed that the predicted downstream development of the boundary layer integral quantities downstream will not be affected, hence providing acceptable accuracy for the calculation of the profile drag. This assumption can be supported by the fact that in this region the flow is encountering a favourable pressure gradient and the growth of the boundary layer is retarded.

Recent studies on AL flow control for form drag reduction has raised concern about the numerical fix as the turbulent flow in the vicinity of the AL is very important for this type of analysis. Therefore, further study is required to validate the LE approximation and/or propose a model applicable immediately downstream of the AL and robust while marching in the region where the numerical fix is currently applied.

4.3. Modification to Leading Edge Model

In Callisto the LE approximation is applied while $\psi \leq 80°$ and from the current experiment

this zone ends somewhere in the region $0.005 < x/c < 0.01$, as shown in Fig. 8. The new experimental results, Fig. 7, show that in this region the limiting streamline angle is restricted to $-4° < \beta < 4°$. Therefore, in the proximity of the AL, $\tan\beta \approx 0$, as β is small, but $\partial\beta/\partial x \neq 0$. Based on this assumption the normal momentum integral equation can be modified and a new set of governing equations derived, for the case of very small β, which are no longer singular within the region previously approximated in Callisto. Once $\tan\beta$ recovers to a finite value the full 3D system of equations can be re-adopted. More details of the derivation of the governing equations are available in reference [6]. The development of the streamwise momentum thickness obtained from the computation with the improved LE modelling (new) can be compared with those from the previous version of Callisto (old) in Fig. 11, where s/c represents the normalised coordinate along the surface of wing profile. The computation with the modified version was conducted for both the geometrical sweep condition set at 60° and the effective sweep which was calculated to be approximately 62° using the experimental static pressure at $x/c=0$.

In Fig. 11, looking at the prediction from the previous version of Callisto, θ remains constant immediately downstream of the AL due to the LE approximation and starts to increase again once a solution of the full governing equations is obtained, at $\psi > 80°$. In the modified version, the full governing equation can be solved immediately downstream of the AL and a comparison between the computed results and experimental results in Fig. 11 shows a significant improvement, as the momentum thickness is now predicted to be within ±5% of the experimental results. The non-monotonic behaviour in the experimental momentum thickness is also now replicated by the numerical results, providing confidence in the experimental observation.

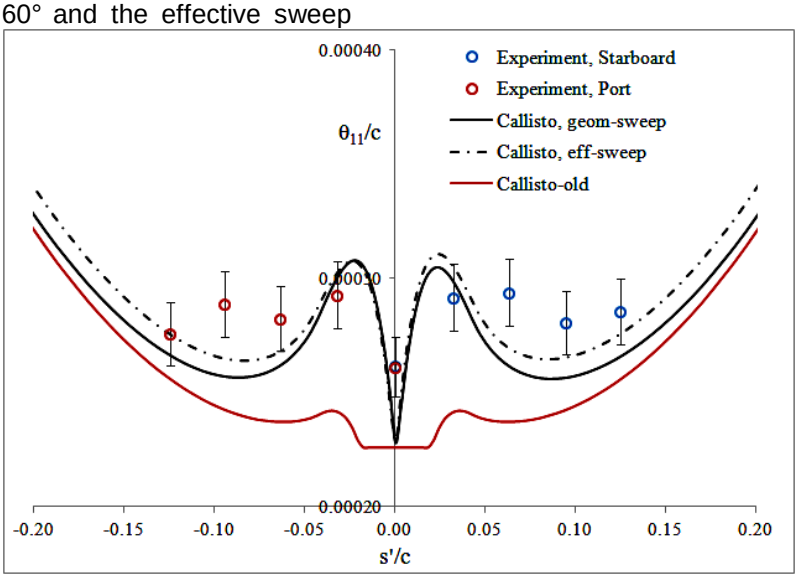

Figure 11: Comparison of θ captured experimentally against those computed using the previous and the modified version of Callisto.

5. DISCUSSION

Fig. 4 shows that, for $R_\theta \geq 315$, the linear region of the velocity profiles collapses onto the modified log-law. This finding is in agreement with Preston's [17] criterion for minimum Reynolds number for the existence of a fully turbulent boundary layer on a flat plate where $R_\theta \approx 320$. Based on this result a new regime where the AL is intermittent can be defined for $100 < R_\theta < 315$. It is our belief that the AL has been previously misinterpreted to be fully turbulent in this regime, which is misleading during flow control studies on swept wings. In addition, on the mid-span and outboard section of the wings of short-haul, and the outboard section of long-haul transonic aircraft $R_\theta < 300$; therefore numerical analysis which assumes fully turbulent flow right from the AL is likely to be incorrect.

The considerable increase in the boundary layer integral quantities immediately downstream of the AL underlines the need for

improved modelling in Callisto. The modified set of governing equations can be considered satisfactory due to the now good agreement between the calculated and the experimental results.

Despite the significant change in the leading edge modelling, the profile drag prediction was not significantly affected as the predicted momentum thickness in the far wake was almost similar from both the old and the new version of Callisto. The revised computational results in Fig. 11 show a rapid growth in momentum thickness downstream of the AL followed by an equally rapid decay, presumably due to the interplay between streamline curvature and favourable pressure gradient at the LE. From the mean flow measurements it is difficult to understand and describe the physical mechanism responsible for the non-monotonic growth in θ in the vicinity of the AL, but as similar trend was predicted by Callisto a simple diagnosis was conducted by analysing the individual terms of the streamwise momentum integral equation. This stationary points in the trend of θ appears when the magnitude of the favourable pressure gradient overtakes the skin friction immediately downstream of the AL, hence slowing the growth in θ, which results in a maximum point. The minimum point is associated with the point where skin friction exceeds the magnitude of the favourable pressure gradient, thus θ grows again. Similar behaviour was also observed for calculation of flow over transonic wing at cruise condition. By $x/c = 0.25$, θ estimated by the modified Callisto has almost merged with that obtained from the previous version, and any residual differences are smaller than the effect of correcting for effective sweep. Based on these observations, the overall profile drag predictions obtained from earlier versions of Callisto can still be considered robust.

The formation of cross-over crossflow profiles in laminar boundary layers is usually associated with a change in sign of the crossflow pressure gradient and an associated inflection point in the external streamline but, from Fig. 8, this explanation cannot be applied to the present, turbulent boundary layer. However, despite the absence of any inflection point in the external streamline, crossover was still present in the crossflow velocity profiles at $x/c > 0.0025$. Following analysis of the transverse momentum equation in curvilinear coordinates, Gowree [6] suggested that along a fully turbulent curved streamline this effect might occur due to the rapid growth in transverse Reynolds stresses, compared to the crossflow pressure gradient, especially at the leading edge of swept wings.
The present experimental results can also be of use for the validation of higher-order turbulence models which are aimed at capturing the effect of lateral strain from highly diverging or converging streamlines.

Finally, although significant improvement in computing power has allowed the modelling of very complicated flow structures by DNS and LES and this has enriched our understanding of the mechanics of fluids, there is still value in maintaining and developing low-order integral boundary layer methods as, due to their rapid turn-around time, they are still considered a useful tool during the design and optimisation of transonic aircraft – provided that the flow predictions are consistent with those obtained from higher-order methods applied later in the design process.

6. CONCLUSION

Measurements at the leading edge of a swept wing model have helped to shed some light on the minimum Reynolds number for a turbulent attachment line which is in agreement with Preston's criterion for the flow on a flat plate. Based on the observed small values of limiting streamline angle, β, near the attachment line, a new approach to solving the 3D momentum integral equations near the attachment line has been implemented in the Airbus Callisto method. The results from the revised method show good agreement with the experimental results, correctly capturing the observed non-monotonic behaviour of θ in this region.

7. ACKNOWLEDMENT

The authors would like to express their gratitude to the Aeromechanics team of Airbus Group Innovations for their financial support.

8. REFERENCES

[1] P. Garabedian and D. Korn, "Analysis of transonic aerofoil," *Communications on Pure and Applied Mathematics,* vol. 24, 1971.

[2] R. C. Lock, "An equivalence law relating three- and two-dimensional pressure distributions.," NPL Aero Report no. 1028, 1962.

[3] J. Green, D. Weeks and J. Brooman, "Prediction of turbulent boundary layers and wakes in compressible flow by lag-entrainment method," ARC R&M, 1973.

[4] P. Ashill, R. Wood and D. Weeks, "An

improved, semi-inverse method of the viscous Garabedian and Korn method (VGK)," RAE Technical Report 87002, 1987.

[5] R. Lock and B. Williams, "Viscous and inviscid interactions in external aerodynamics," *Progress in Aerospace Science,* vol. 24, 1987.

[6] E. R. Gowree, "Influence of Attachment Line on Form Drag," PhD Thesis, City University London, 2014.

[7] J. H. Preston, "The Determination of Turbulent Skin Friction by Means of Pitot Tubes," Journal of Royal Aeronautical Society, vol. 58, 1954.

[8] Pfenninger W, "Flow Phenomena at the Leading Edge of Swept wings, Recent development in Boundary Layer Research," AGARDograph 97, 1965.

[9] M. Gaster, "On the flow along swept leading edges," *Aeronautical Quarterly,* vol. 17, 1967.

[10] Cumpsty N A and Head M R, "The Calculation of the Three-Dimensional Turbulent Boundary Layer. Part III: Comparison of the Attachment Line Calculations with Experiment," *Aeronautical Quarterly,* vol. 20, 1969.

[11] P. R. Spalart, "Direct Simulation of a Turulent Boundary layer up to R=1410," vol. 187, 1988.

[12] J. P. Johnston, "On the three dimensional boundary layer generated by secondary flows," ASME, Journal of Fluid Engineering, vol. 82, 1960.

[13] C. J. Atkin and E. R. Gowree, "Recent Development to the Viscous Garabedian and Korn Method," 28th International Congress of the Aeronautical Sciences, Brisbane, 2012.

[14] C. J. Atkin, "Summary of the Swept-Tapered Lag-Entrainment Boundary Layer Method in Callisto version 3.4," Technical Report QinetiQ/08/00064, 2008.

[15] P. Smith, "A calculation method for the turbulent Boundary layer on an infinite yawed wing in compressible , adiabatic flow," ARC. CP. 1268, 1974.

[16] B. G. J. Thompson. B. G. J. and G. J. McDonald, "The prediction of boundary layer behaviour and profile drag for infinite swept wings: Part III a method for calculation," ARC CP 1309, 1973.

[17] J. H. Preston, "The Mininmum Reynolds Number for a Turbulent Boundary Layer and the Selection Transition Device," Journal of Fluid Mechanics, vol. 3, 1957.